MAS cryoprobe enhances solid-state NMR signals of α-synuclein fibrils

Malitha C. Dickwella Widanage,[a, b, c] Barbara Perrone,[d] Jhinuk Saha,[a, b, c] Riqiang Fu,[a] Jochem Struppe,[e] Ryan P. McGlinchey,[f] Jennifer C. Lee,[f] Robert W. Schurko,[a, g] and Ayyalusamy Ramamoorthy[*a, b, c,h]

Here, we report on the enhanced sensitivity of solid-state NMR experiments on α-synuclein fibrils using a MAS cryoprobe. Nearly an order of magnitude improvement in signal-to-noise was observed in CPMAS, refocused-INEPT and 2D ^{13}C-^{13}C chemical shift correlation spectra of α-synuclein fibrils acquired using a MAS cryoprobe compared to that of a conventional MAS probe.

Solid-state NMR (ssNMR) spectroscopy is widely used for atomistic-resolution structural studies of a variety of solids. Magic-angle spinning (MAS) combined with recoupling techniques has become a standard approach for characterizing the structure and dynamics of amyloid fibrils.[1-3] While many high-resolution structures of amyloid fibrils have been reported, the investigation of lowly populated or heterogeneous amyloid species remains challenging due to the inherently low sensitivity of ssNMR. Although dynamic nuclear polarization (DNP) can enhance the sensitivity,[4-6] room-temperature measurements are often preferred for studying dynamic species and maintaining native-like sample conditions. In this context, the recently developed MAS cryoprobe for solid-state NMR offers a valuable alternative by significantly enhancing the sensitivity and without the need to freeze the sample.[7,8]

In this study, we report ssNMR results acquired using a MAS cryoprobe on uniformly ^{13}C- and ^{15}N-labeled α-synuclein (α-syn) fibrils formed in the presence of 500 mM NaCl. α-Syn fibril deposition is a key pathological feature of neurodegenerative disorders such as Parkinson's disease, dementia with Lewy bodies, and multiple system atrophy.[9,10] Importantly, α-syn fibrils are classified as amyloids, adopting cross-β structure, stabilized by hydrogen-bond networks of amide backbones, steric zippers, and salt bridges, as determined by ssNMR[11,12] and other high-resolution techniques.[13-18] Fibril structural characterization is critical to understanding disease mechanisms as recent studies indicate a possible relationship between distinct fibril polymorphs and disease phenotypes.[11,19-23]

Since α-syn fibrils are highly polymorphic and concentrations of these structural variants differ within a sample, it becomes challenging to study them by ssNMR. Spectral line-broadening hampers resolution, and more critically, low-abundance amyloid species remain undetected. However, ssNMR experiments performed using a MAS cryoprobe, without the need to freeze the sample, have been shown to enhance sensitivity, thereby potentially enabling the detection of minor amyloid species in heterogeneous mixtures.

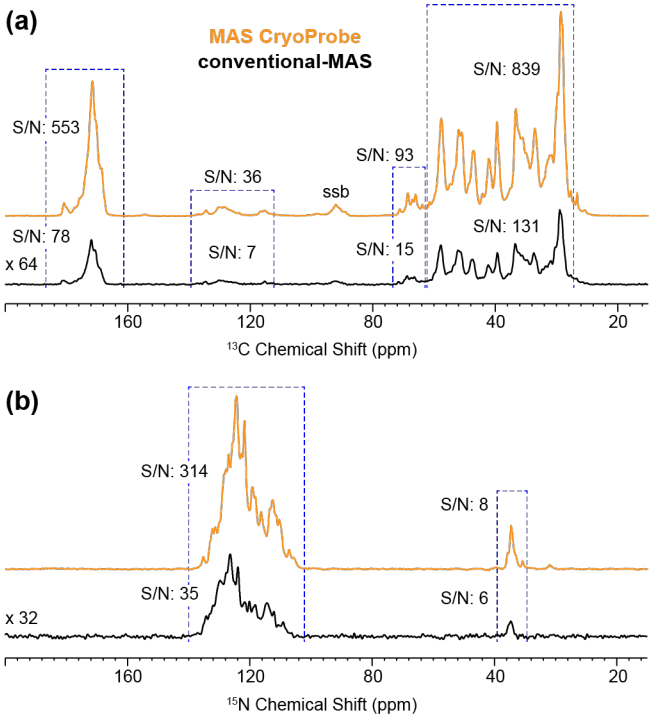

Fig. 1 MAS cryoprobe enhances the sensitivity for both ^{13}C- and ^{15}N-detection. (a) ^{13}C CPMAS spectra and (b) ^{15}N CPMAS spectra acquired using a MAS cryoprobe (Bruker, yellow) and a conventional 3.2 mm HCN MAS probe (home-built at the MagLab, black). Measurements were performed on a 600 MHz spectrometer at 12 kHz MAS and 268 K with ~1 mg of α-syn fibrils. All NMR parameters are given in Supplementary Table 1.

[a.] *National High Magnetic Field Laboratory, 1800 E. Paul Dirac Drive, Tallahassee, FL 32310, United States.*
[b.] *Department of Chemical and Biomedical Engineering, FAMU-FSU College of Engineering, Tallahassee, FL 32310, United States.*
[c.] *Institute of Molecular Biophysics, Florida State University, Tallahassee, FL 32304*
[d.] *Bruker Biospin, Fällanden, Switzerland.*
[e.] *Bruker, Billerica, United States.*
[f.] *Laboratory of Protein Conformation and Dynamics, Biochemistry and Biophysics Center, National Heart, Lung, and Blood Institute, National Institutes of Health, Bethesda, MD 20892, United States*
[g.] *Department of Chemistry and Biochemistry, Florida State University, Tallahassee, FL 32306, United States.*
[h.] *Biophysics and Department of Chemistry, University of Michigan, Ann Arbor, MI 48109, United States.*
Current address: M.C.D.Widanage, Renewable Resources and Enabling Sciences Center, National Renewable Energy Laboratory, Golden, CO, 80401, United

In this study, we compare ssNMR spectra obtained using a MAS cryoprobe with those acquired using a conventional MAS probe under identical experimental conditions. The performance of a 3.2 mm HCN MAS cryoprobe (from Bruker) was benchmarked against the conventional 3.2 mm HCN MAS probe (home-built MagLab) for solid-state NMR of ~1 mg α-syn fibrils. ^{13}C and ^{15}N-labeled α-syn was expressed and purified as reported elsewhere,[24] and the fibril samples were prepared as described in the Supporting Information. 1D ^{13}C and ^{15}N cross-polarization (CP) experiments were performed at 600 MHz (14.1 T) under 12 kHz MAS at 268 K (**Fig. 1**). The use of MAS cryoprobe provided significantly enhanced sensitivity, allowing the acquisition of high-quality two-dimensional spectra with a reduced experimental time as explained below.

As shown in **Fig. 1**, the data collected with the MAS cryoprobe (yellow traces) exhibit pronounced sensitivity improvements for both ^{13}C and ^{15}N nuclei. The ^{13}C MAS spectra (**Fig. 1a**) show that weak aliphatic (~65 to 75 ppm) and aromatic (~105 to 135 ppm) resonances are better resolved in the spectrum acquired using the MAS cryoprobe. Quantitative signal-to-noise (S/N) analysis yields a sensitivity gain of about 6 for ^{13}C, which is in excellent agreement with previously reported gains for similar experiments using a MAS cryoprobe.[18] Similarly, the ^{15}N CP spectra (**Fig. 1b**) demonstrate a remarkable ~9-fold S/N enhancement when using a MAS cryoprobe, facilitating the detection of amide signals that are barely discernible in the spectrum acquired using the conventional probe. The improved sensitivity reflects the reduced thermal noise and the enhanced cryogenic preamplifier efficiency of the MAS cryoprobe design, which is particularly advantageous for low-γ nuclei like ^{15}N and for samples available in limited quantities.

The MAS cryoprobe provided pronounced enhancements in both signal sensitivity and spectral resolution for 2D ^{13}C-^{13}C correlation experiments. As illustrated in **Fig. 2a**, spectra acquired with a 50 ms DARR mixing time using the MAS cryoprobe demonstrate substantially higher S/N ratio relative to those obtained using a conventional MAS probe under identical acquisition parameters (NS = 32). Remarkably, even with minimal signal averaging (NS = 2), the MAS cryoprobe spectrum retains comparable, or even better, spectral details, emphasizing the significant reduction in experimental time afforded by MAS cryoprobe (**Fig. 2b**). The application of a QSINE apodization function during Fourier transformation further improved spectral quality by attenuating truncation artifacts while preserving intrinsic resolution.[8,25]

To further demonstrate the sensitivity and resolution gains obtained with MAS cryoprobe, selected 1D slices extracted from 2D spectra are shown in **Fig. 2b**. Notably, the enhanced resolution enables the discrimination of five distinct peaks, whereas the conventional MAS probe yields only three broadened and unresolved resonances (14–22 ppm). Expanded views of the highlighted spectral regions

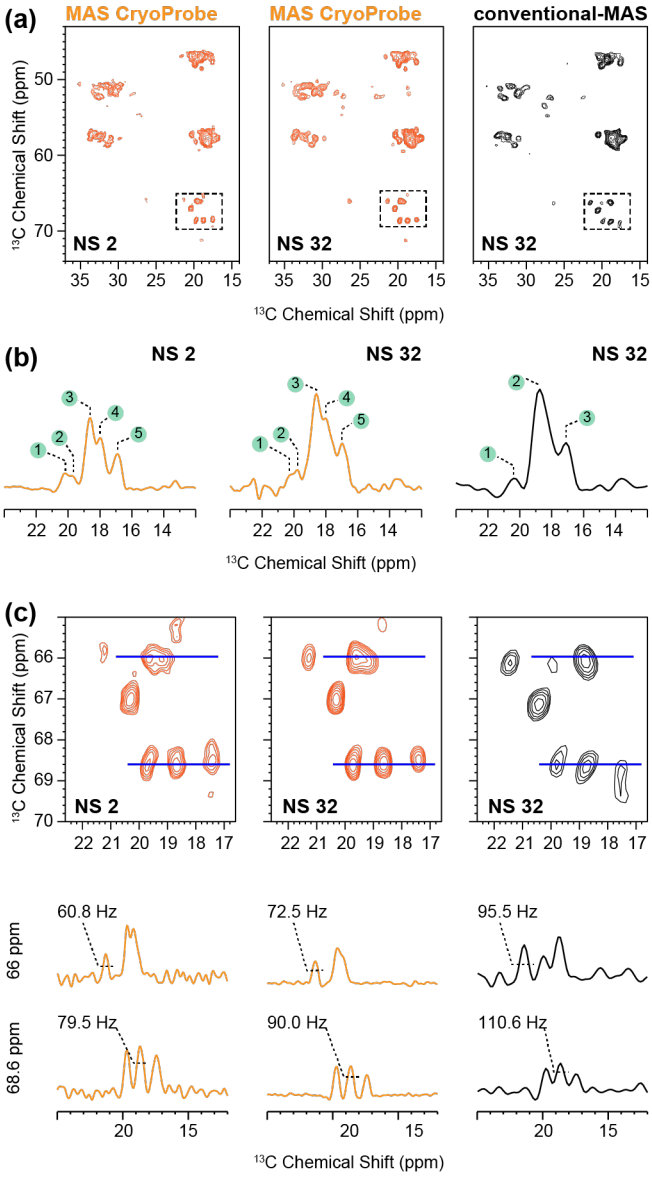

Fig. 2 Signal enhancement and improved resolution with MAS cryoprobe. 2D ^{13}C-^{13}C spectra acquired with 50 ms DARR (a) using a MAS cryoprobe (left: number of accumulated scans (NS) = 2; middle: NS = 32) and a conventional MAS probe (right: NS = 32), processed with a QSINE apodization function. Selected 1D slices (b) at 57.8 ppm demonstrate the enhanced sensitivity and resolution achieved with MAS cryoprobe. Expanded views (c) of 2D spectral regions (highlighted with dashed line box), with blue lines indicating the positions of additional 1D slices at 66.0 ppm and 68.6 ppm. Full width at half maximum (FWHM) values are provided for selected peaks to illustrate resolution differences. All the NMR and processing parameters used to obtain these spectra are given in Supplementary Table 1.

(**Fig. 2c**) further reveal narrow linewidths in spectra acquired with the MAS cryoprobe, as quantified by full width at half maximum (FWHM) values for peaks at 66.0 ppm and 68.6 ppm. While a cryoprobe does not inherently provide higher spectral resolution, the improved resolution observed in Fig.2 is likely a consequence of the enhanced S/N.

Employing a MAS cryoprobe yields a marked enhancement in spectral sensitivity and retention of long-range ^{13}C-^{13}C correlations in 2D DARR experiments at extended mixing times. As shown in **Fig.3a**, the 250 ms DARR spectrum acquired with a MAS cryoprobe exhibits substantially higher cross-peak intensities and S/N compared to that obtained with the conventional MAS probe, reflecting the improved detection sensitivity afforded by the cryoprobe.[22] The ability to detect weak dipolar-driven magnetization transfers during long mixing periods enables the observation of inter-residue and distal intra-residue correlations. Extracted 1D traces along the direct (t2) and indirect (t1) dimensions (**Fig. 3b** and **3c**, respectively) highlight the enhanced dynamic range and resolution achievable due to the enhanced S/N rendered by a MAS cryoprobe. This sensitivity gain would be valuable for the complete mapping of structural connectivity in complex solid-state systems, particularly for aliphatic and aromatic spin systems where cross-peak intensities are inherently low.

The ^{13}C refocused-INEPT spectra acquired with the MAS cryoprobe also exhibit a pronounced sensitivity enhancement, particularly in the aliphatic region, compared to that obtained using a conventional MAS probe (**Fig. 4**). Refocused-INEPT selectively can be used to selectively detect mobile molecular components (or regions of a protein), by using scalar (J) coupling-based coherence transfer that is efficient only in segments undergoing fast motion. Consequently, it emphasizes flexible aliphatic chains, dynamic side groups, and mobile carbohydrate or lipid moieties whose signals are typically attenuated in CP-based experiments due to weak ^{1}H-^{13}C dipolar coupling. The first FID obtained from the 2D refocused-INEPT based 2D

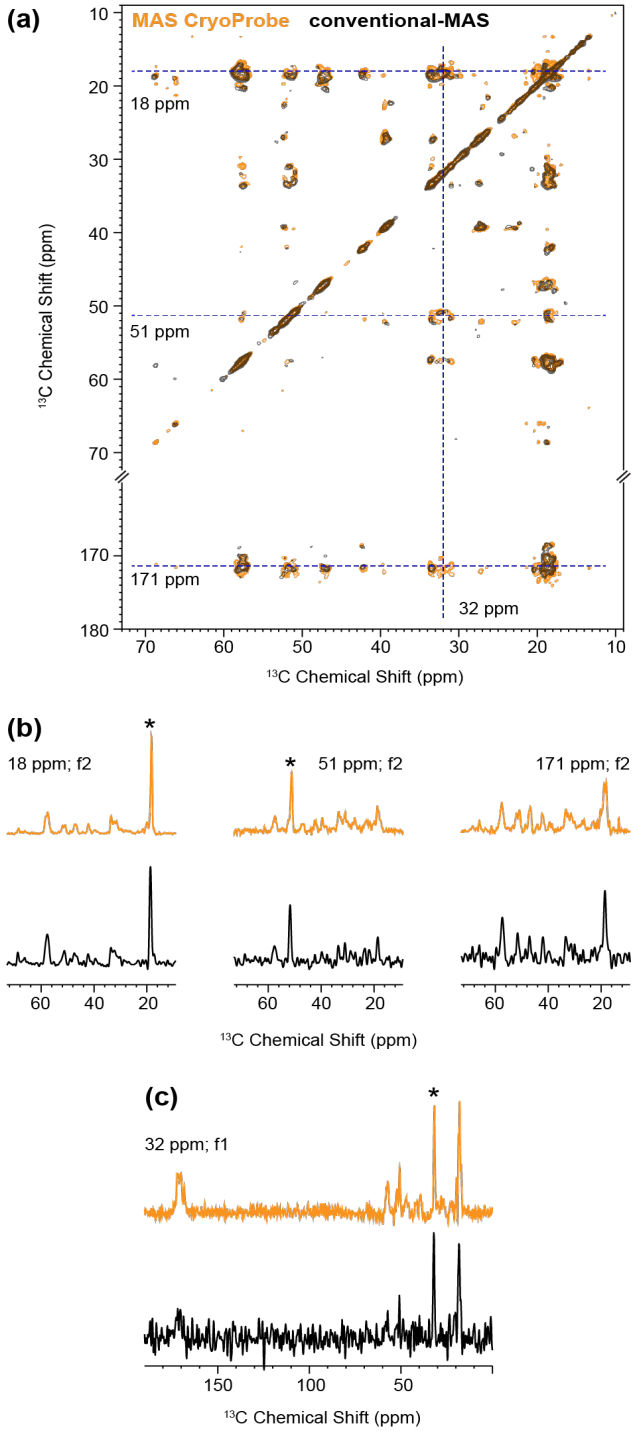

Fig. 3 Long mixing time preserves signal intensity with MAS cryoprobe. 2D ^{13}C-^{13}C 250 ms DARR spectra acquired using MAS cryoprobe and, conventional MAS probes (a). (b and c) Selected 1D slices extracted at the frequencies marked by blue dashed lines are shown for the direct (t2) and the indirect (t1) dimensions. Spectra illustrate enhanced cross-peak retention and sensitivity in MAS cryoprobe. All the NMR and processing parameters are given in Supplementary Table 1. * denotes the diagonal peak.

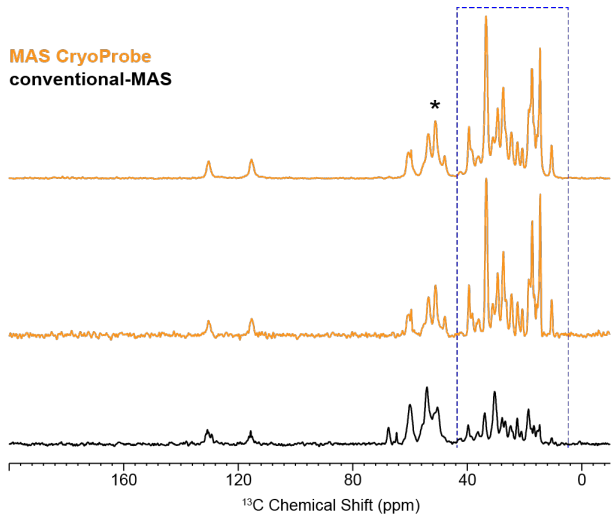

Fig. 4 Enhanced sensitivity in the aliphatic region with MAS cryoprobe. 1D ^{13}C refocused-INEPT spectra acquired using MAS cryoprobe (top) along with the 1st FID of the 2D $^{1}H/^{13}C$ HETCOR from MAS cryoprobe (middle), and 1D ^{13}C refocused-INEPT spectrum acquired using conventional MAS probe (bottom),. All spectra were locally normalized to the region indicated by asterisks to highlight relative signal enhancement. All the NMR parameters used to acquire these spectra are given in Supplementary Table 1.

$^{1}H/^{13}C$ HETCOR experiment acquired with MAS cryoprobe (bottom) exhibits higher S/N, further illustrating the enhanced performance of MAS cryoprobe for the detection of dynamic components in the sample (**Supplementary Fig. 1**).

In summary, our results demonstrate the impact of cryogenic probe technology for solid-state NMR applications, particularly in systems where sample quantity is limited or nuclei of inherently low receptivity, such as ^{15}N, are of interest. The enhanced sensitivity directly translates into reduced experimental time or improved spectral resolution through additional signal averaging.

Acknowledgements: This study was funded by the NIH (R01DK132214 to A.R.). The work performed at NHMFL is supported by National Science Foundation Cooperative Agreement No. DMR-2128556* and the State of Florida. This research was supported in part by the Intramural Research Program of the National Institutes of Health (NIH). The contributions of the NIH authors are considered Works of the United States Government. The findings and conclusions presented in this paper are those of the authors and do not necessarily reflect the views of the NIH or the U.S. Department of Health and Human Services.

Conflicts of interest

There are no conflicts to declare.

Data availability

Materials and methods, supplementary figures and additional experimental data are included in the Supporting Information. Experimental data files are available at the *Open Science Framework*:https://osf.io/3k9v8/?view_only=962b2a565973422eae64bfa2463165df

Notes and references

1 Jaroniec CP, MacPhee CE, Bajaj VS, McMahon MT, Dobson CM, Griffin RG. Proceedings of the National Academy of Sciences. 2004;101(3):711-6.
2 Colvin MT, Silvers R, Frohm B, Su Y, Linse S, Griffin RG. High resolution structural characterization of Aβ42 amyloid fibrils by magic angle spinning NMR. Journal of the American Chemical Society. 2015;137(23):7509-18.
3 Comellas G, Rienstra CM. Protein structure determination by magic-angle spinning solid-state NMR, and insights into the formation, structure, and stability of amyloid fibrils. Annual review of biophysics. 2013;42:515-36.
4 Sergeyev IV, Fritzsching K, Rogawski R, McDermott A. Resolution in cryogenic solid-state NMR: Challenges and solutions. Protein Science. 2024;33(7): e4803.
5 Tycko R. NMR at low and ultralow temperatures. Accounts of chemical research. 2013 Sep 17;46(9):1923-32.
6 Lopez del Amo JM, Schneider D, Loquet A, Lange A, Reif B. Cryogenic solid state NMR studies of fibrils of the Alzheimer's disease amyloid-β peptide: perspectives for DNP. Journal of biomolecular NMR. 2013;56(4):359-63.
7 Vallet A, Ayala I, Perrone B, Hassan A, Simorre JP, Bougault C, Schanda P. MAS NMR experiments of corynebacterial cell walls: Complementary ^{1}H- and MAS CryoProbe-enhanced ^{13}C-detected experiments. J Magn Reson. 2024;364:107708.
8 Hassan A, Quinn CM, Struppe J, Sergeyev IV, Zhang C, Guo C, Runge B, Theint T, Dao HH, Jaroniec CP, Berbon M, Lends A, Habenstein B, Loquet A, Kuemmerle R, Perrone B, Gronenborn AM, Polenova T. Sensitivity boosts by the MAS CryoProbe for challenging biological assemblies. J Magn Reson. 2020 Feb;311:106680.
9 Spillantini MG, Crowther RA, Jakes R, Hasegawa M, Goedert M. α-Synuclein in filamentous inclusions of Lewy bodies from Parkinson's disease and dementia with Lewy bodies. Proceedings of the National Academy of Sciences. 1998 26;95(11):6469-73.
10 Wakabayashi K, Hayashi S, Kakita A, Yamada M, Toyoshima Y, Yoshimoto M, Takahashi H. Accumulation of α-synuclein/NACP is a cytopathological feature common to Lewy body disease and multiple system atrophy. Acta neuropathologica. 1998;96(5):445-52.
11 Dhavale DD, Barclay AM, Borcik CG, Basore K, Berthold DA, Gordon IR, Liu J, Milchberg MH, O'Shea JY, Rau MJ, Smith Z. Structure of alpha-synuclein fibrils derived from human Lewy body dementia tissue. Nature communications. 2024;15(1):2750.
12 Tuttle MD, Comellas G, Nieuwkoop AJ, Covell DJ, Berthold DA, Kloepper KD, Courtney JM, Kim JK, Barclay AM, Kendall A, Wan W. Solid-state NMR structure of a pathogenic fibril of full-length human α-synuclein. Nature structural & molecular biology. 2016;23(5):409-15.
13 Ni X, McGlinchey RP, Jiang J, Lee JC. Structural insights into α-synuclein fibril polymorphism: effects of Parkinson's disease-related C-terminal truncations. Journal of molecular biology. 2019;431(19):3913-9.
14 McGlinchey RP, Ni X, Shadish JA, Jiang J, Lee JC. The N terminus of α-synuclein dictates fibril formation. Proceedings of the National Academy of Sciences. 2021;118(35):e2023487118.
15 Guerrero-Ferreira R, Taylor NM, Arteni AA, Kumari P, Mona D, Ringler P, Britschgi M, Lauer ME, Makky A, Verasdonck J, Riek R. Two new polymorphic structures of human full-length alpha-synuclein fibrils solved by cryo-electron microscopy. Elife. 2019;8:e48907.
16 Li Y, Zhao C, Luo F, Liu Z, Gui X, Luo Z, Zhang X, Li D, Liu C, Li X. Amyloid fibril structure of α-synuclein determined by cryo-electron microscopy. Cell research. 2018;28(9):897-903.
17 Li B, Ge P, Murray KA, Sheth P, Zhang M, Nair G, Sawaya MR, Shin WS, Boyer DR, Ye S, Eisenberg DS. Cryo-EM of full-length α-synuclein reveals fibril polymorphs with a common structural kernel. Nature communications. 2018;9(1):3609.
18 Guerrero-Ferreira R, Taylor NM, Mona D, Ringler P, Lauer ME, Riek R, Britschgi M, Stahlberg H. Cryo-EM structure of alpha-synuclein fibrils. elife. 2018 Jul 3;7:e36402.
19 Schweighauser M, Shi Y, Tarutani A, Kametani F, Murzin AG, Ghetti B, Matsubara T, Tomita T, Ando T, Hasegawa K, Murayama S. Structures of α-synuclein filaments from multiple system atrophy. Nature. 2020;585(7825):464-9.
20 Yang Y, Shi Y, Schweighauser M, Zhang X, Kotecha A, Murzin AG, Garringer HJ, Cullinane PW, Saito Y, Foroud T, Warner TT. Structures of α-synuclein filaments from human brains with Lewy pathology. Nature. 2022;610(7933):791-5.
21 Scheres SH, Ryskeldi-Falcon B, Goedert M. Molecular pathology of neurodegenerative diseases by cryo-EM of amyloids. Nature. 2023;621(7980):701-10.
22 Yang Y, Garringer HJ, Shi Y, Lövestam S, Peak-Chew S, Zhang X, Kotecha A, Bacioglu M, Koto A, Takao M,

Spillantini MG. New SNCA mutation and structures of α-synuclein filaments from juvenile-onset synucleinopathy. Acta Neuropathologica. 2023;145(5):561-72.
23 Shahnawaz M, Mukherjee A, Pritzkow S, Mendez N, Rabadia P, Liu X, Hu B, Schmeichel A, Singer W, Wu G, Tsai AL. Discriminating α-synuclein strains in Parkinson's disease and multiple system atrophy. Nature. 2020;578(7794):273-7.
24 McGlinchey RP, Ramos S, Dimitriadis EK, Wilson CB, Lee JC. Defining essential charged residues in fibril formation of a lysosomal derived N-terminal α-synuclein truncation. Nature Communications. 2025 Apr 23;16(1):3825.
25 Holmes JB, Liu V, Caulkins BG, Hilario E, Ghosh RK, Drago VN, et al. Imaging active site chemistry and protonation states: NMR crystallography of the tryptophan synthase α-aminoacrylate intermediate. Proceedings of the National Academy of Sciences. 2022;119(2): e2109235119.